Salen-Manganese Complexes: Sophisticated Tools for the Analysis of Intercellular ROS Signaling Pathways

STEFANIE J. OPHOVEN and GEORG BAUER

Department of Virology, Institute for Medical Microbiology and Hygiene, University of Freiburg, D-79104 Freiburg, Germany

Abstract. *Salen-manganese complexes, such as EUK-8 and EUK-134 are known as catalase mimetics with superoxide dismutase (SOD) and peroxidase mimetic activity. Here we show that the concentration-dependent use of salen-manganese complexes within the appropriate time window and with parallel control of signaling parameters allows complex interactions during intercellular induction of apoptosis to be studied. At very low concentrations, salen-manganese complexes can abrogate consumption reactions between HOCl and hydrogen peroxide, as well as NO and hydrogen peroxide, and thus the major signaling pathways are enhanced. At higher concentrations of the compounds, all major signaling pathways are inhibited, thereby the catalase mimetic activity of the compounds affects both hydrogen peroxide and peroxynitrite. The ratio between available hydrogen peroxide and salen-manganese complexes defines whether reactive oxygen species (ROS) effects are inhibited or apoptosis is induced by the compounds. The SOD mimetic activity of salen-manganese complexes seems to be insufficient to interfere with intercellular ROS signaling.*

Activation of membrane-associated NADPH oxidase (NOX-1) is functionally connected to oncogenic transformation (1-5). Extracellular superoxide anions generated by NOX-1 and their dismutation product hydrogen peroxide are crucial for the control of proliferation, maintenance of the transformed state and tumor progression (1-3, 5-8). However, superoxide anions also drive specific elimination of transformed cells through reactive oxygen species (ROS)-mediated intercellular induction of apoptosis (9-13). Here the term 'ROS' comprises classical reactive oxygen species such as superoxide anions, HOCl, hydrogen peroxide and hydroxyl radicals, as well as reactive nitrogen species such as nitric oxide (NO) and peroxynitrite. During ROS-mediated intercellular induction of apoptosis, superoxide anion-generating transformed cells represent the 'target cells', whereas nontransformed 'effector cells' contribute to intercellular induction of apoptosis through the release of a novel peroxidase (POD) and NO (Figure 1). As transformed cells also exhibit effector cell functions (release of POD and/or NO), the interaction of target and effector functions of transformed cells can establish autocrine, ROS-mediated apoptotic signaling (14) (Figure 1). The interaction of nontransformed and transformed cells, as well as the autocrine interaction of transformed cells, establishes the same four ROS signaling pathways that cause selective apoptosis in transformed target cells (for review see references 12-15). Thereby, the HOCl (11) and the NO/peroxynitrite signaling pathway (4, 11) are the dominant pathways, whereas the nitryl chloride pathway (16) and the metal-catalyzed Haber-Weiss reaction (17) seem to be of minor importance. The chemical details of the HOCl and the NO/peroxynitrite signaling pathway are described in Figure 1. Whereas transformed cells are regularly sensitive to intercellular ROS signaling, *ex vivo* tumor cells exhibit resistance towards this process (14, 18). Their resistance was shown to be based on interference of catalase located outside of the cell membrane with intercellular ROS signaling (14, 19, 20). Thereby catalase was shown to decompose hydrogen peroxide, as well as peroxynitrite, efficiently, and thus to interfere with all four intercellular ROS-mediated signaling pathways (20). During the last years, the development of synthetic superoxide dismutase (SOD) and catalase mimetics has been pursued (21). In the course of these approaches, salen-manganese complexes, a group of cell-permeable, low-molecular weight agents, have been found to show promising activity. Their non-proteinaceous nature, their catalytic mode of action, as well as their distinctive property of mimicking both SOD and catalase enzymatic function (22-26), indicating a broad pharmacological potential, raised high expectations for their therapeutic effect in a wide range of

Correspondence to: Georg Bauer, Abteilung Virologie, Institut für Medizinische Mikrobiologie und Hygiene, Hermann-Herder Strasse 11, D-79104 Freiburg, Germany. e-mail: georg.bauer@uniklinik-freiburg.de

Key Words: Reactive oxygen species, intercellular signaling, apoptosis, salen-manganese complex.

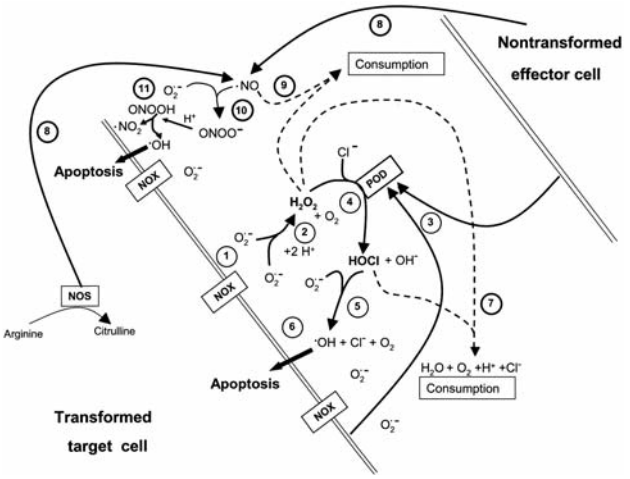

Figure 1. *Intercellular ROS signaling between nontransformed and transformed cells and autocrine apoptosis induction in transformed cells. Transformed target cells exhibit activated NADPH oxidase (NOX-1) in their membrane and generate extracellular superoxide anions (#1). Superoxide anions dismutate spontaneously to hydrogen peroxide and oxygen (#2). Transformed as well as nontransformed effector cells release duox-coded peroxidase (#3). This release is triggered by TGF-β (not shown). Peroxidase (POD) utilizes hydrogen peroxide and chloride anions to synthesize HOCl (#4). HOCl then interacts with superoxide anions in the vicinity of the transformed target cell membrane, thereby yielding hydroxyl radicals (#5) that cause lipid peroxidation in the membrane (#6). Lipid peroxidation is followed by ceramide generation, activation of the mitochondrial pathway of apoptosis, activation of caspases 9 and 3, followed by apoptosis (details not shown). In the case of excess hydrogen peroxide compared to POD, hydrogen peroxide and HOCl interact in the consumption reaction shown under (#7). This consumption reaction inhibits HOCl signaling. NO synthase (NOS; either iNOS, nNOS or eNOS, depending on the cell system) in target and effector cells utilizes the substrate arginine to synthesize NO (#8). NO readily permeates cellular membranes. It may be consumed by hydrogen peroxide in a complex consumption reaction (#9) that will be described in detail elsewhere. Alternatively, NO interacts with superoxide anions to form peroxynitrite (#10). Peroxynitrite can be protonated to peroxynitrous acid that spontaneously decomposes into NO_2 and apoptosis inducing hydroxyl radicals (#11). For clarity, the two minor signaling pathways, i.e. the nitryl chloride pathway and the metal-catalyzed Haber-Weiss reaction have not been included. The nitrylchloride pathway utilizes HOCl that interacts with nitrite to form apoptosis-inducing nitryl chloride. The metal-catalyzed Haber-Weiss reaction depends on hydrogen peroxide that reacts with ferrous ions to yield hydroxyl radicals and hydroxyl anions. The resulting ferric ions are then reduced by superoxide anions back to ferrous ions that undergo the next cycle. In contrast to transformed cells, tumor cells are protected against intercellular ROS signaling through expression of membrane-associated catalase (14, 19, 20) (not shown). Catalase decomposes hydrogen peroxide and thus blocks HOCl signaling, as well as the nitryl chloride pathway and the metal-catalyzed Haber-Weiss reaction. Catalase also efficiently decomposes peroxynitrite and thus blocks the NO/peroxynitrite pathway. In addition, catalase intermediate* $CATFe^{IV}=O^{+}$. *(compound I) can oxidize NO to* NO_2 *and thus counteract peroxynitrite formation.*

oxidative and nitrosative stress-related disease states. The development of these effective compounds also offered new perspectives for the analysis of complex ROS signaling processes. Salen-manganese complexes such as the prototype *N,N'-bis*(salicylidene) ethylenediamine chloride (EUK-8) contain a coordinated manganese ion whose status determines whether the complex functions as an SOD or catalase mimetic (27). The mechanism employed for the dismutation of superoxide anions is very similar to that of MnSOD. In a first step, Mn(III) is reduced to Mn(II) by a superoxide anion, releasing molecular oxygen. The Mn(II) is then converted back to Mn(III) by another superoxide anion, yielding water. In the context of its catalase mimetic activity, salen-manganese is oxidized to a salen-oxomanganese complex by hydrogen peroxide, liberating water. The initial complex is then regenerated, detoxifying another molecule of hydrogen peroxide thereby releasing water and molecular oxygen. In addition to their SOD and catalase mimetic activity, EUK compounds have also been found to scavenge hypochlorous acid and peroxynitrite (27), to oxidize nitric oxides (27) and to exhibit peroxidase activity (24). Here we demonstrate how salen-manganese complexes enable clear analysis of complex interactions between components of intercellular ROS signaling, when appropriate parallel controls are performed and the concentration of the compounds is well controlled.

Materials and Methods

Materials. Diethylammonium (Z)-1-(N,N-diethylamino)diazen-1-ium-1,2-diolate (DEA-NONOate) was obtained from Sigma Aldrich (Schnelldorf Germany), dissolved at a final concentration of 200 mM stock solution in medium and stored at –20˚C. Care was taken to minimize the time between preparation of the stock solution (on ice) and freezing the aliquots and between thawing the aliquots and their addition to the assays. DEA-NONOate represents a rapidly decaying NO-donor with a half-life time of 2 minutes at 37˚C. Manganese N,N'-bis(salicylidiene)ethylenediamine chloride (EUK-8) was obtained from Calbiochem/Merck Chemicals Ltd (Nottingham, UK) and was dissolved in dimethyl sulfoxide (DMSO) at a concentration of 1 M and was then diluted with medium to a concentration of 10 mM (stock solution). The stock solution was kept at –20˚C. EUK-8 is a synthetic salen-manganese complex with high SOD and catalase-mimic activities. Control experiments ensured that the minute concentration of DMSO brought into the assay had no effect. Chloro[[2,2'-[1,2-ethanediyl*bis*[(nitrilo-κ*N*)methylidyne]]*bis*[6-methoxyphenolato-κO]]-manganese (EUK-134), a cell-permeable synthetic salen-manganese complex, was obtained from Cayman chemicals (Ann Arbor, Michigan, USA). EUK-134 was dissolved in DMSO to reach a concentration of 1 M and was then immediately diluted in EMEM containing 5% fetal bovine serum (FBS) (Biochrome, Berlin, Germany) to a final concentration of 10 mM. This stock solution was stored at –20˚C. Control assays ensured that the residual DMSO concentrations had no interfering effect on ROS signaling. 5-, 10-, 15-, 20-Tetrakis(4-sulfonatophenyl)porphyrinato iron(III) chloride) (FeTPPS), a specific decomposition catalyst for peroxynitrite, was obtained from Calbiochem/Merck Chemicals Ltd. Stock solutions (10 mM) were kept at –20˚C. Specificity control experiments ensured that FeTPPS effectively decomposed peroxynitrite but that it did not affect hydrogen peroxide or

superoxide anions. Glucose oxidase (GOX), from *Aspergillus niger*, (Sigma Aldrich), generates hydrogen peroxide using glucose as substrate. Glucose is present in abundance in Eagle's Minimal Essential Medium (EMEM) and RPMI-1640 media (Biochrome). GOX was kept as 6,000 U/ml stock solution at 4˚C. Manganese(III)-5,10,15,20-tetrakis(*N*-methylpyridinium-2-yl)porphyrin pentachloride (MnTM-2-PyP), a cell-permeable SOD mimetic and decomposition catalyst for peroxynitrite, was obtained from Calbiochem/Merck Chemicals Ltd. and kept as 10 mM stock solution in phosphate buffered saline (PBS) at –20˚C. NaOCl was obtained from Sigma Aldrich. The stock solution of 860 mM was kept at 4˚C in the dark. As the pKa of OCl– is 7.64, the majority of the species are present as HOCl at neutral pH. For simplicity, the term 'HOCl' is used through out this paper. HOCl was diluted in cold, sterile PBS and then added to the assays as a single aliquot (10-20 µl per 100 µl assay). Care was taken to add HOCl at a similar speed and from the same distance above the medium in order to avoid differences in local concentration of HOCl immediately after addition. Peroxynitrite (synthesized from isoamylnitrite and hydrogen peroxide) was obtained as a 200 mM stock solution from Calbiochem/Merck Chemicals Ltd. It was kept at –70˚C until use. Cu-SOD from bovine erythrocytes was obtained from Sigma Aldrich. Stock solutions (30,000 Units/ml in PBS) were kept at –20˚C and only used once per aliquot. Cu-SOD is an efficient scavenger of superoxide anions. Xanthine oxidase (XO) and xanthine were obtained from Sigma Aldrich. When XO was applied in the experiments, the medium contained 0.4 mM xanthine. XO generates superoxide anions. Transforming growth factor β1 (TGF-β1) was purified from human platelets (28) and kept as a stock solution of 1.5 µg/ml in EMEM plus 5% FBS at –20˚C.

Media for cell culture. Cells were either kept in EMEM, containing 5% fetal bovine serum or in RPMI 1640 medium, containing 10% FBS, as indicated for the respective cell lines. FBS had been heated for 30 minutes at 56˚C prior to use. Both media were supplemented with penicillin (40 U/ml), streptomycin (50 µg/ml), neomycin (10 µg/ml), moronal (10 U/ml) and glutamine (280 µg/ml) from Sigma Aldrich. Cell culture was performed in plastic tissue culture flasks. Cells were passaged once or twice weekly.

Cell lines. Transformed 208Fsrc3 cells exhibit constitutive expression of *v-src* and have been established in the laboratory of R. Schäfer, Berlin, Germany. 208Fsrc3 cells show criss cross morphology, form colonies in soft agar and are sensitive to intercellular induction of apoptosis (10, 14). 208Fsrc3 cells were cultured in EMEM medium containing 5% FBS. The human gastric carcinoma cell line MKN-45 was obtained from the DSMZ, Braunschweig, Germany. The cells were grown in RPMI 1640 medium, containing 10% FBS.

Autocrine apoptosis induction in transformed cells. 208Fsrc3 cells, 12,500 in 100 µl EMEM, containing 5% FBS and 20 ng/ml TGF-β1, were seeded in 96-well tissue culture clusters and then further incubated at 37˚C in a humidified incubator at 5% CO_2. Under these conditions, apoptosis is specifically induced in transformed cells, dependent on their own intercellular ROS signaling, as described in Figure 1. Additional compounds for modulation and analysis of this process, as indicated in the legends to Figures 2-5, were added after the cells had attached. This time point was set as time zero of the experiment. At the indicated time, the percentages of apoptotic cells were determined as described below.

NO/peroxynitrite-mediated apoptosis induction. 208Fsrc3 cells, 12,500 in 100 µl EMEM, containing 5% FBS and 20 ng/ml TGF-β1, were seeded in 96-well tissue culture clusters. After the cells had attached, either the rapidly decaying NO donor DEA-NONOate (that interacts with transformed cell-derived extracellular superoxide anions to form peroxynitrite) or exogenous peroxynitrite were added and the assays were incubated at 37˚C in a humidified incubator at 5% CO_2 until the quantification of the percentages of apoptotic cells. Under these conditions, apoptosis induction is driven by the exogenous compounds (DEA-NONOate or peroxynitrite) in a reaction that is faster than autocrine apoptosis induction by itself.

Quantification of extracellular superoxide anion generation. 208Fsrc3 cells, 12,500 in 100 µl EMEM, containing 5% FBS and 20 ng/ml TGF-β1, were seeded per well in 96-well tissue culture clusters. After the cells had attached, the assays received the indicated concentrations of the compounds to be tested, or no addition. Serial dilutions of Cu-SOD, as indicated, were then added to the assays. Finally, 0.5 mM DEA-NONOate were added to all assays. The percentages of apoptotic cells were determined after 4 h. The quantification of the relative concentrations of extracellular superoxide anions is based on the interaction of cell-derived extracellular superoxide anions with NO released by DEA-NONOate, resulting in peroxynitrite-mediated apoptosis induction. Cu-SOD, in a concentration-dependent mode, initially blocks this reaction through removal of superoxide anions and prevention of peroxynitrite formation. As soon as the point of maximal inhibition has been reached, addition of more Cu-SOD leads to a gradual increase of excess SOD-Cu^+ molecules (the intermediates of the SOD reaction). As free superoxide anions are not available under these conditions, the SOD-Cu^+ intermediate cannot complete the SOD reaction cycle and rather reduces NO to nitroxyl anions (NO^-). These interact with molecular oxygen and generate peroxynitrite. This results in an increase in apoptosis induction with increasing high concentrations of Cu-SOD. In total, the interaction of Cu-SOD with DEA-NONOate-mediated apoptosis induction in transformed cells results in a bell-shaped curve with a distinct point of maximal inhibition. Calibration experiments (not shown) have demonstrated that an increase in available extracellular superoxide anions causes a rightward shift, a decrease causes a leftward shift. The increase in the concentration of free superoxide anions is directly proportional to the increase of Cu-SOD necessary to reach the point of maximal inhibition. This increase can thus be taken as a measure for the relative change in superoxide anion concentration. Quantitation of extracellular superoxide anion generation requires parallel controls to assure that the cells do not show apoptosis above background in the absence of the NO donor (data not shown).

Quantification of apoptosis induction. Determination and quantification of apoptosis was based on the classical morphological criteria of membrane blebbing, nuclear condensation and nuclear fragmentation. These were determined by using inverted phase contrast microscopy as recently described (14, 20). The percentage of apoptotic cells was determined from at least 200 cells categorized per assay. Apoptotic cells were either attached or rounded and showed: a) membrane blebbing, or b) membrane blebbing and nuclear condensation/fragmentation or c) membrane fragmentation/condensation without blebbing (these cells seem to represent later stages of apoptosis where the blebs have been already lost). Care was taken to differentiate apoptotic cells from nonapoptotic rounded cells with intact nuclei, reflecting mitotic stages.

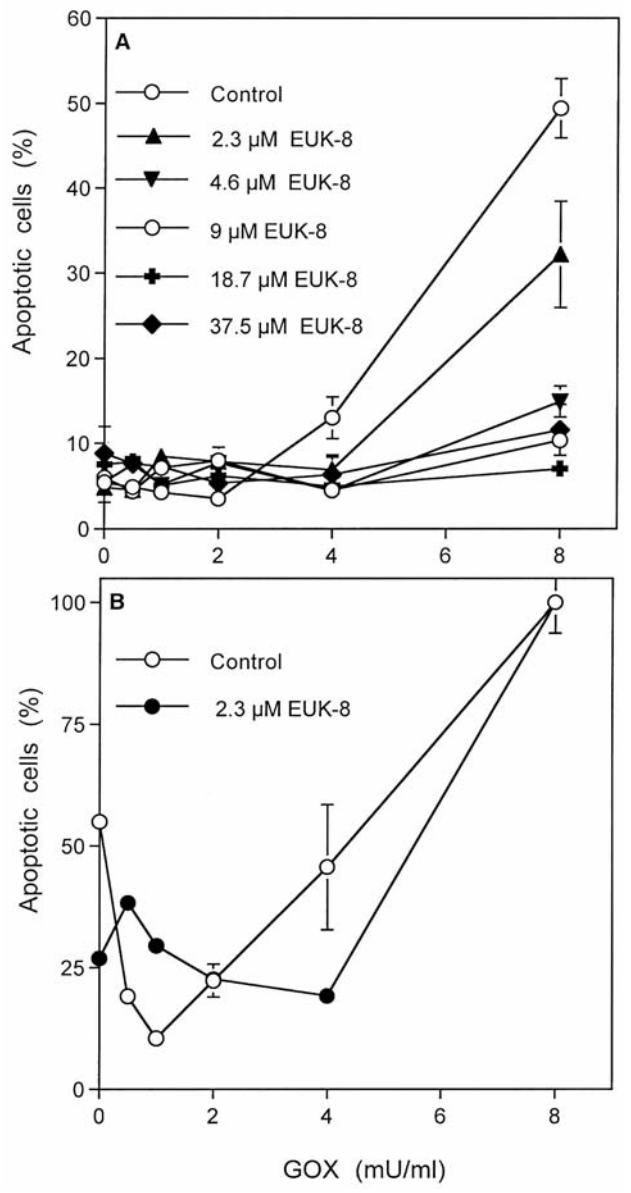

Figure 2. *Catalase mimetic activity of EUK-8. The indicated concentrations of the hydrogen peroxide-generating enzyme glucose oxidase and the catalase mimetic EUK-8 were added to assays for autocrine apoptosis induction. Controls did not receive EUK-8. The percentages of apoptotic cells were determined after 4 h (A) and 27.5 h (B).*

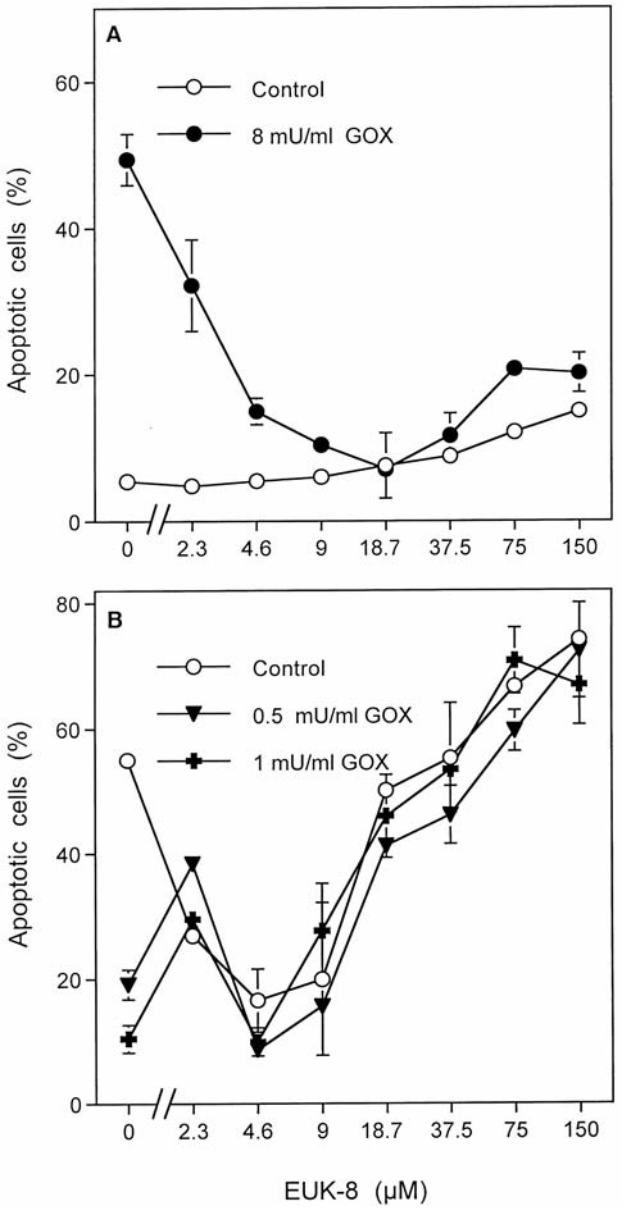

Figure 3. *Dependency of EUK-8 catalase mimetic activity on its concentration. The indicated concentrations of GOX and the catalase mimetic EUK-8 were added to assays for autocrine apoptosis induction. Controls did not receive EUK-8. The percentages of apoptotic cells were determined after 4 h (A) and 27.5 h (B).*

Statistical analysis. In all experiments, assays were performed in duplicate. The mean values (from duplicate assays within the same experiment) and the empirical standard deviations were calculated and are shown in the figures. Absence of standard deviation bars for certain points indicates that the standard deviation was too small to be reported by the graphic program, *i.e.* that results obtained in parallel were nearly identical. Empirical standard deviations were calculated merely to demonstrate how close the results were obtained in parallel assays within the same experiment and not with the intention of statistical analysis of variance, which would require larger numbers of parallel assays. Key experiments were repeated more than five times, involving different investigators. The Yates continuity-corrected Chi-square test was used for the statistical determination of significances. As rather broad concentration ranges are used in our studies, the presentation of the data required logarithmic abscissae in the case of Figures 3-7 and 9-11.

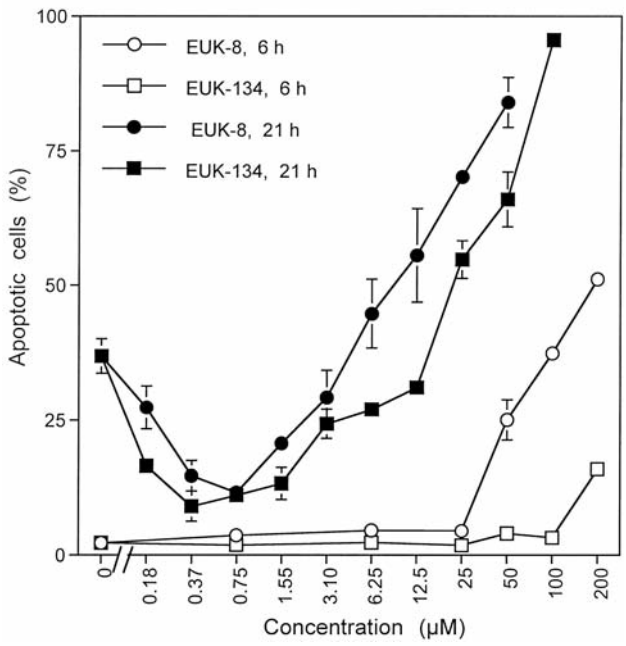

Figure 4. *Protective and destructive action of EUK-8 and EUK-134 on 208Fsrc3 cells. The indicated concentrations of EUK-8 or EUK-134 were added to assays for autocrine apoptosis induction. The percentages of apoptotic cells were determined after 6 and 21 h. Please note that EUK-8 and EUK-134 at low concentrations inhibit autocrine apoptosis induction but cause rapid and strong apoptosis induction when applied at high concentrations.*

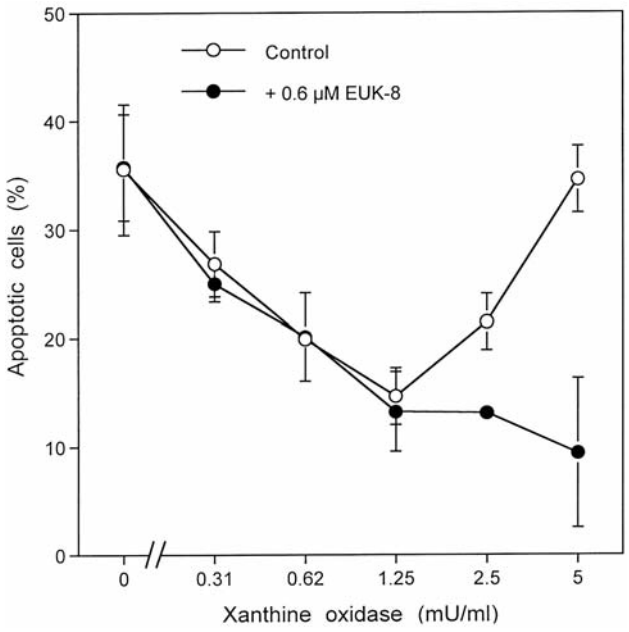

Figure 5. *Effect of EUK-8 on the interaction of xanthine oxidase with autocrine apoptosis induction. The indicated concentrations of xanthine oxidase, in the absence or presence of 0.6 μM EUK-8, were added to assays for autocrine apoptosis induction, supplemented with 0.4 mM xanthine. The percentages of apoptotic cells were determined after 25 h.*

Results

The first experiments aimed to define the usefulness of the catalase mimetic activity of EUK-8 for the analysis of complex signaling reactions, in which hydrogen peroxide is involved in multiple ways: i) direct apoptosis induction by hydrogen peroxide, a rather rapid process with no selectivity with respect to the transformed or nontransformed state of cells; ii) autocrine apoptosis induction, a process selectively carried out by transformed cells, in which hydrogen peroxide is used as substrate for HOCl synthesis, and iii) inhibition of HOCl signaling by hydrogen peroxide through consumption of HOCl. Src oncogene-transformed fibroblasts were incubated with increasing concentrations of hydrogen peroxide-generating GOX, in the absence or presence of increasing concentrations of the catalase mimetic EUK-8. After 4 h of incubation, the transformed cells did not yet show autocrine apoptosis induction, but high concentrations of GOX had induced apoptosis (Figure 2A). This direct apoptosis-inducing effect of hydrogen peroxide was efficiently prevented by EUK-8 in a concentration-dependent mode. EUK-8 at 4.6 μM had a strong inhibitory effect and at 18.7 μM it caused a complete inhibition of hydrogen peroxide-dependent apoptosis induction. After 27.5, *src* oncogene-transformed cells, in the absence of GOX and EUK-8, exhibited autocrine apoptosis induction. Small concentrations of GOX blocked autocrine apoptosis induction, whereas higher concentrations of GOX restored direct apoptosis induction by hydrogen peroxide (Figure 2B). EUK-8 at 2.3 μM inhibited autocrine apoptosis induction of transformed cells, confirming the dependence of this process on available hydrogen peroxide. EUK-8 at this concentration also counteracted the inhibition of autocrine apoptosis induction by small concentrations of GOX, confirming the role of hydrogen peroxide in this complex inhibition reaction; 2.3 μM EUK-8 showed an inhibitory effect against 4 mU/ml GOX but not against 8 mU/ml GOX. The analysis of the concentration-dependence of EUK-8 action (Figure 3) demonstrates that higher concentrations of EUK-8 were required to completely block fast direct apoptosis induction by 8 mU/ml GOX compared to lower concentrations of EUK-8 required for the slower process of autocrine apoptosis induction of transformed cells. Already at 4 h, very high concentrations of EUK-8 indicated the establishment of an optimum curve of inhibition, with 18.75 μM EUK-8 representing the optimum.

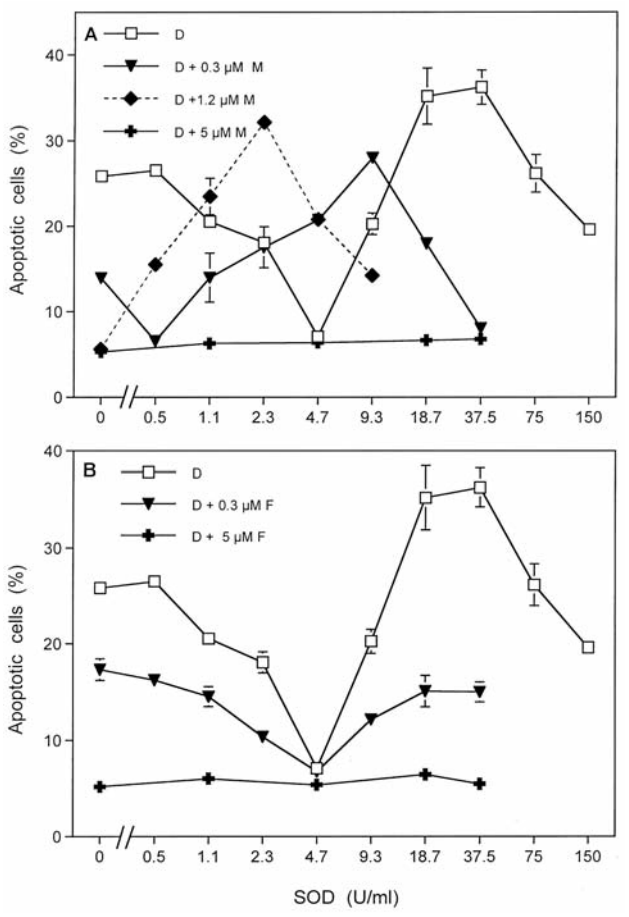

Figure 6. *Effect of the SOD mimetic MnTM-2-PyP (positive control) and the peroxynitrite decomposition catalyst FeTPPS (negative control) on free superoxide anion concentration. Assays for the quantification of extracellular superoxide anion generation received the indicated concentrations of MnTM-2-PyP (M) (Figure 6A) or FeTPPS (F) (Figure 6B) in the presence of 0.5 mM of the NO donor DEA-NONOate (D). The percentages of apoptotic cells were determined after 4 h. Please note that the SOD mimetic MnTM-2-PyP caused a leftward shift of the bellshaped inhibition curve, indicative for a proportional decrease of superoxide anions, before it completely inhibited apoptosis induction. FeTPPS caused no shift of the bell-shaped inhibition curve with respect to the concentration of Cu-SOD, but caused a concentration-dependent inhibition of apoptosis through decomposition of peroxynitrite.*

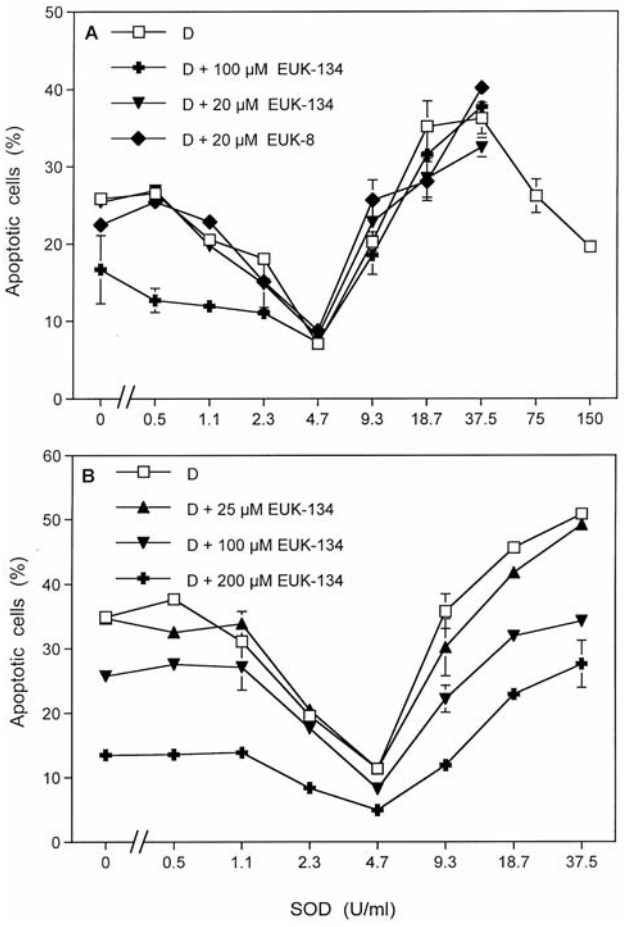

Figure 7. *EUK-8 and EUK-134 have no effect on free superoxide anion concentration. The indicated concentrations of EUK-8 and EUK-134 were tested together with 0.5 mM DEA-NONOate (D) in the assay for quantification of extracellular superoxide anion generation. DEA-NONOate without EUK-8 or EUK-134 represents the reference curve (D). There was no indication for an effect of the two compounds on the concentration of free superoxide anions.*

At 27.5 h, a rather complex picture of interaction was seen. In the absence of GOX, autocrine apoptosis induction was inhibited by EUK-8, with an optimum of inhibition at 4.6 μM EUK-8. Higher concentrations of EUK-8 caused massive apoptosis induction at this time point. Low concentrations of GOX blocked autocrine apoptosis induction. This inhibitory effect was partially abrogated by 2.3 μM EUK-8. At 4.6 μM EUK-8, the partially reconstituted reaction was blocked again and higher concentrations of EUK-8 caused strong apoptosis induction at that time point. A more detailed study of the effects of low concentrations of EUK-8 showed that 0.6 μM EUK-8 completely abrogated the inhibitory effect of 0.5 mU/ml GOX without affecting autocrine apoptosis induction itself (data not shown). The results shown in Figure 4 confirm that EUK-8 and the related compound EUK-134 inhibited autocrine apoptosis induction of transformed cells at very low concentrations and induced apoptosis markedly at higher concentrations. Apoptosis induction by high concentrations of these compounds was already detectable at 6 h when autocrine apoptosis induction was not yet occurring. Therefore, a fine tuned application of EUK-8 or EUK-34 should be useful for the characterization of hydrogen peroxide-mediated processes, but an additional apoptosis effect of high concentrations of the mimetics has

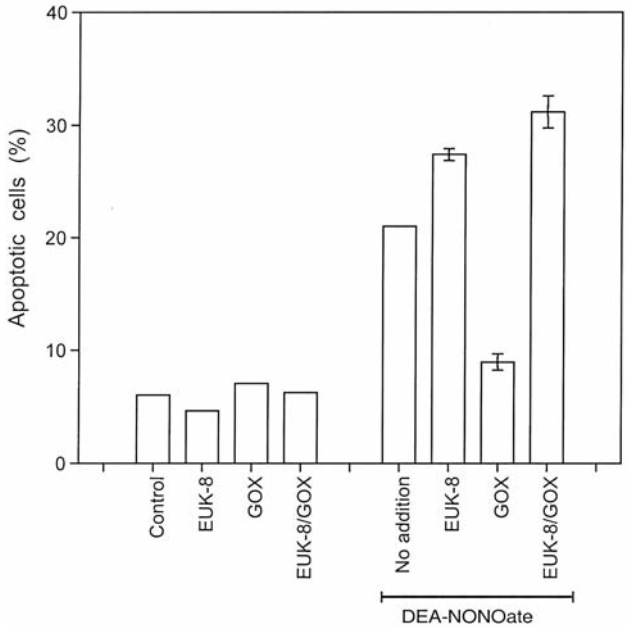

Figure 8. *The inhibitory effect of hydrogen peroxide on NO-mediated apoptosis induction is abrogated by EUK-8. Assays for NO/peroxynitrite-mediated apoptosis induction remained free of additions (control) or received either 2 μM EUK-8, or 2 mU/ml GOX or a combination of GOX and EUK-8. Assays were performed both in the absence and presence of 0.03 mM DEA-NONOate. The percentages of apoptotic cells were determined after 3 h.*

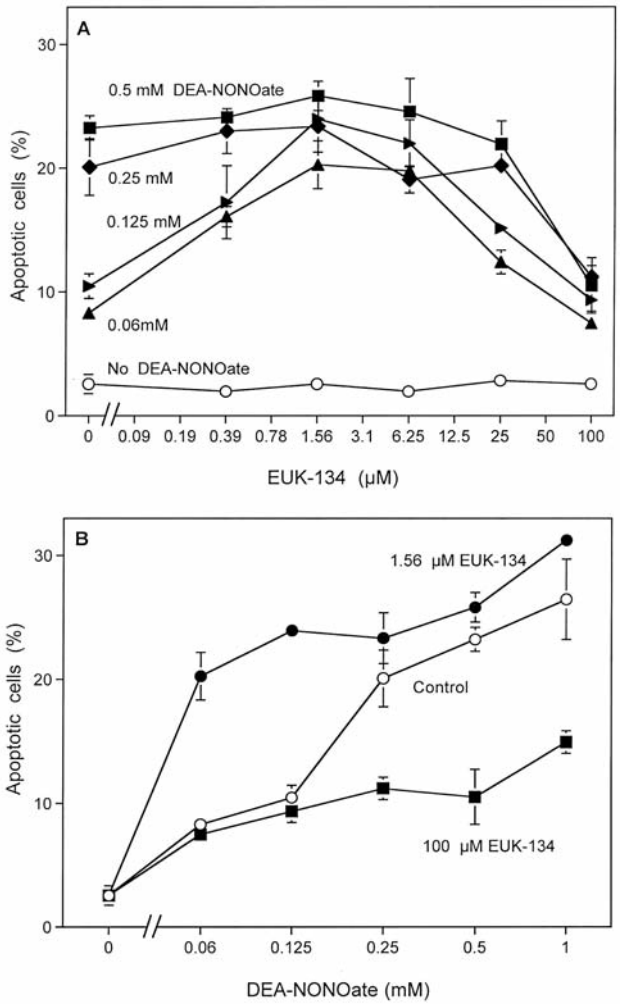

Figure 9. *Dual effect of EUK-134 on NO-mediated apoptosis induction in transformed cells. Assays for NO/peroxynitrite-mediated apoptosis induction received the indicated concentrations of DEA-NONOate and EUK-134. The percentages of apoptotic cells were determined after 4 h. A) Apoptosis induction according to EUK-134 concentrations, in the absence or the presence of DEA-NONOate. B) Apoptosis induction according to DEA-NONOate concentrations, in the absence or presence of EUK-134.*

to be taken into consideration. For the evaluation of the analytical potential of salen-manganese compounds in complex ROS signaling interactions, the interference of XO with autocrine apoptosis induction was used (Figure 5). XO, in the presence of xanthine or hypoxanthine generates superoxide anions which dismutate to hydrogen peroxide. The inhibition of autocrine apoptosis induction by XO up to 1.25 mU/ml might be caused by the interaction between XO-derived superoxide anions and HOCl distant from the cell membrane, thus blunting the HOCl signaling pathway. Alternatively, hydrogen peroxide generated by dismutation of XO-derived superoxide anions might interact with HOCl and cause inhibition of HOCl signaling in this way. The resumed apoptosis induction at 2.5 and 5 mU/ml XO was likely to represent a hydrogen peroxide-dependent process, as superoxide anions do not cause apoptosis induction by themselves. EUK-8 at a concentration of 0.6 μM did not influence autocrine apoptosis induction. Inhibition of autocrine apoptosis by XO up to 1.25 mU/ml was not influenced by 0.6 μM EUK-8 at all, whereas apoptosis induction by XO at 2.5 and 5 mU/ml was completely inhibited by EUK-8. This finding indicates that the inhibitory effect on autocrine apoptosis induction in the smaller concentration range of XO is not mediated by hydrogen peroxide and is thus different from the effect observed for GOX (Figure 3), and therefore seems to represent an effect of superoxide anions. In contrast, apoptosis induction at higher concentrations of XO seems to represent an effect of the dismutation product hydrogen peroxide. EUK-8 has been reported to interact with superoxide anions as well (21, 22) and thus to exhibit an SOD-analogous activity. We endeavoured to find out whether this activity is of relevance or potential use in the analysis of ROS signaling. For the quantification of relative changes in extracellular superoxide anion concentration, we

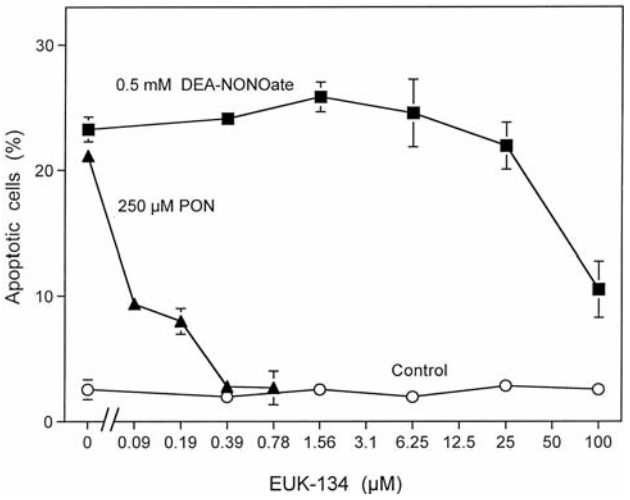

Figure 10. *Protective effect of EUK-8 against peroxynitrite-induced apoptosis. Assays for NO/peroxynitrite-mediated apoptosis induction received the indicated concentrations of EUK-134. Parallel assays remained free of further additions or 250 µM peroxynitrite (PON) or 0.5 mM DEA-NONOate were added. The percentages of apoptotic cells were determined after 4 h. Please note that both apoptosis induction after direct addition of PON or after action of the NO donor is mediated by PON. In the case of addition of the NO donor, PON is exclusively formed close to the membrane of the transformed cells through interaction of NO with extracellular superoxide anions.*

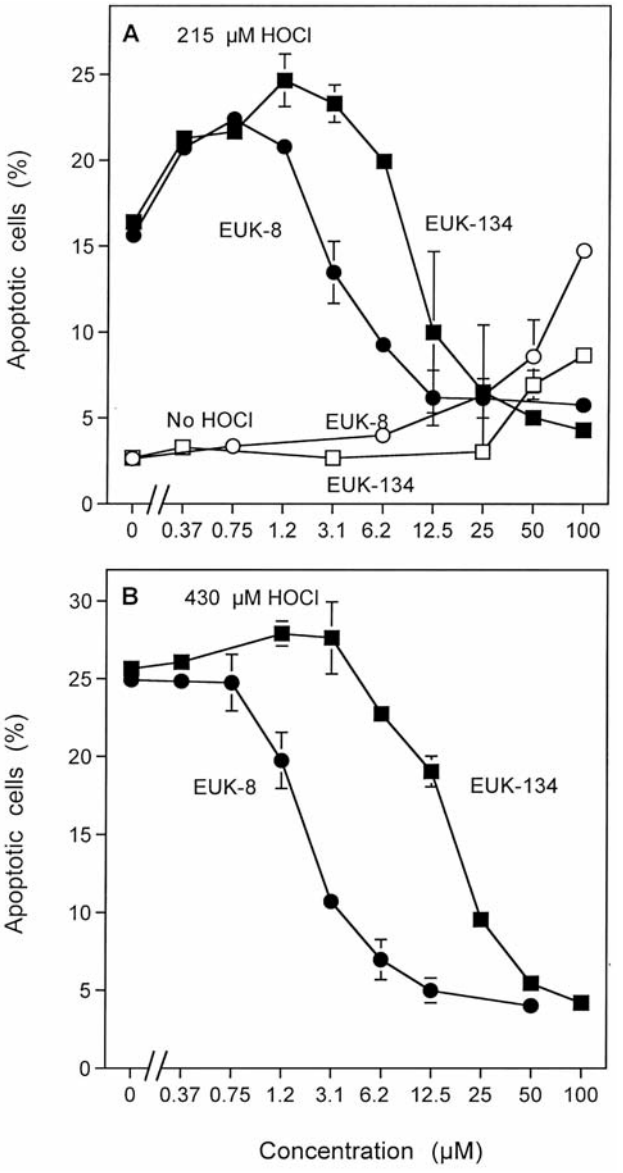

Figure 11. *Decomposition of HOCl by EUK-8 and EUK-134. Human gastric carcinoma MKN-45 cells (8,000), were seeded per well (96-well tissue culture cluster) in 100 µl medium, containing 5% FBS. The indicated concentrations of EUK-8 or EUK-134 were added. The assays remained free of further additions or received 215 µM (A) or 430 µM HOCl (B). The percentages of apoptotic cells were determined after 1.5 h.*

used a test system recently established by our group. It is based on apoptosis induction in transformed cells after addition of an NO donor such as DEA-NONOate. NO and cell-derived superoxide anions form peroxynitrite that acts as final apoptosis inducer. Therefore, this process can be blocked by SOD. When Cu-SOD is used, a bell-shaped inhibition curve is observed. The resumed increase of apoptosis after the point of maximal inhibition is due to relative abundance of SOD over superoxide anions in this concentration range of SOD applied. This leads to SOD-Cu+ molecules that do not find a second superoxide anion for completion of the reaction cycle, but that rather interact with NO. As a result, nitroxyl anions are formed and these react with molecular oxygen, thereby generating peroxynitrite that drives apoptosis induction. Any modulation of the concentration of free superoxide anions has been shown to shift the point of maximal inhibition together with the bell-shaped curve (data not shown). Figure 6 A demonstrates that small concentrations of the SOD mimetic MnTM2PyP cause the expected inhibition of the reaction and a shift of the inhibition curve as well. MnTM2PyP at 0.3 µM caused a shift over an eight-fold concentration of SOD. When 1.2 µM MnTMPyP was applied, apoptosis induction in the absence of SOD was completely blocked, but with increasing SOD concentration, the right side of the bell-shaped curve was still clearly detectable. 5 µM of the SOD mimetic caused a complete inhibition of apoptosis induction. This positive control (Figure 6A) is contrasted by FeTPPS which is a potent peroxynitrite decomposition catalyst without SOD mimetic activity. As seen in Figure 6 B, FeTPPS inhibited apoptosis on both sides of the bell-shaped curve without change of the point of maximal inhibition, indicating that peroxynitrite

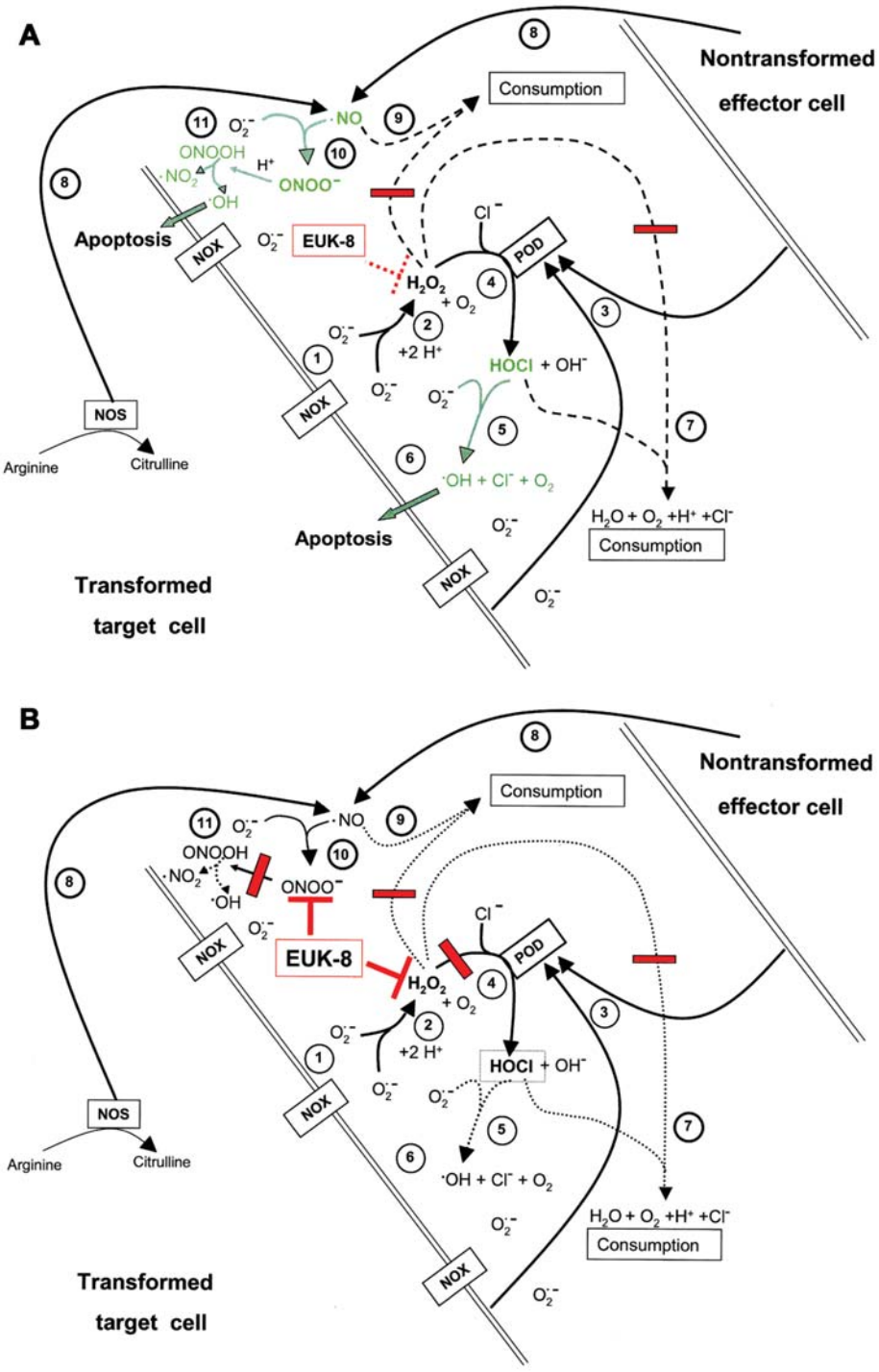

Figure 12. *The use of salen-manganese complexes for the analysis of ROS-mediated intercellular apoptosis signaling. A) Effects of very low concentrations of salen-manganese complexes on intercellular ROS signaling: abrogation of consumption reactions and enhancement of intercellular signaling. Low concentrations of salen-manganese complexes can determined such that the consumption reactions between hydrogen peroxide and HOCl or hydrogen peroxide and NO are abrogated and major signaling pathways are enhanced. B) Effects of moderate and high concentrations of salen-manganese complexes on intercellular signaling: interference with major signaling pathways. Concentrations of salen-manganese complexes can be determined that block the major signaling pathways. Thereby, the decomposition of peroxynitrite formed at the cell membrane through interaction of superoxide anions and NO requires higher concentrations of salen-manganese complexes than the inhibition of HOCl signaling. Please note that decomposition of peroxynitrite that is added to the medium only requires low concentrations of salen-manganese complexes to become decomposed. The figure does not show the potential of salen-manganese complexes to decompose HOCl and their potential to cause toxic effects through HOCl signaling.*

was decomposed without interference with available superoxide anion concentration. When EUK-8 or EUK-134 were applied in this assay at a concentration of 20 μM, they showed neither inhibition of apoptosis nor a shift of the point of maximal inhibition (Figure 7A). This indicates that the compounds at this concentration neither interfered with peroxynitrite nor with superoxide anions. When the concentration of EUK-134 was increased to 200 μM (Figure 7B), inhibition on both sides of the bell-shaped curve was seen, but no shift of the point of maximal inhibition was observed. This result demonstrates the lack of action of EUK-134 towards superoxide anions in our cell system, but shows its potential to interfere with a peroxynitrite-mediated process. There are multiple and complex ways of interactions between reactive oxygen and nitrogen species. We tried to determine whether the salen-manganese complexes are useful tools for a dissection of interacting processes in this area. We have recently shown that consumption of NO by a hydrogen peroxide-dependent process has a strong negative impact on apoptotic signalling by NO *via* peroxynitrite formation. To demonstrate this effect, 0.03 mM DEA-NONOate was added to transformed cells in the absence or presence of 2 mU/ml GOX, 2 μM EUK-8, or a combination thereof. As shown in Figure 8, DEA-NONOate caused apoptosis induction that was dependent on superoxide anion interaction of NO and peroxynitrite formation (as shown in the previous figures). GOX at 2 mU/ml caused nearly complete inhibition of NO-mediated apoptosis. Inhibition by GOX was completely abrogated by 2 μM EUK-8. In the absence of exogenous GOX, EUK-8 enhanced DEA-NONOate-mediated apoptosis induction, indicating that cell-derived hydrogen peroxide was also sufficiently inhibitory. For a further clarification of this point, increasing concentrations of DEA-NONOate were added to src-transformed cells in the absence or presence of increasing concentrations of EUK-134. As shown in Figure 9 A, the apoptosis-mediating effect of low concentrations of DEA-NONOate was first enhanced by increasing concentrations of EUK-134, before inhibition of the process when more than 6 μM EUK-134 was present. The stimulatory effect of EUK-134 was only marginal for higher concentrations of DEA-NONOate, but the inhibitory effect was the same. At 100 μM EUK-8, inhibition of more than 50% was reached. This finding can be interpreted as inhibition of the consumption reaction between NO and hydrogen peroxide at low EUK concentrations and possibly decomposition of peroxynitrite at higher concentrations of EUK-134. The interaction of EUK-134 with NO-mediated apoptosis induction becomes even more clear when apoptosis induction is pictured in response to DEA-NONOate in the absence of EUK-134 and in the presence of the stimulatory concentration of 1.56 μM or the inhibitory concentration of 100 μM (Figure 9B). Stimulation by 1.56 μM EUK-134 is more pronounced in the low concentration range of DEA-NONOate, whereas inhibition by 100 μM EUK-8 has the opposite trend. To further substantiate this aspect, increasing concentrations of EUK-134 were added to transformed cells in the presence of 250 μM peroxynitrite. As seen in Figure 10, the salen-manganese complexes were able to completely inhibit peroxynitrite-induced apoptosis. The concentration of EUK-134 needed for protection was much higher when peroxynitrite was not added directly but was formed at the membrane of the transformed cells through superoxide anion/NO interaction. This interesting steric issue will be addressed later. Salen-manganese complexes have also been reported to interact with HOCl (27). To clarifiy the significance of this potential for the application of the compounds as tools in our signaling system, increasing concentrations of EUK-8 or EUK-134 were used with 215 μM or 430 μM HOCl, or without addition of HOCl. As shown in Figure 11, the apoptosis-inducing effect of 215 μM HOCl was first enhanced and then completely inhibited by EUK-8 and EUK-134. The enhancing effect was not observed for 430 μM HOCl, but inhibition was as effective. The decomposition effect on HOCl was stronger for EUK-8 compared to EUK-134.

Discussion

Our data show that the salen-manganese complexes EUK-8 and EUK-134 represent sophisticated and useful tools for the analysis of complex intercellular ROS signaling, provided their concentration is used in an appropriate range for a specific situation and parallel controls give further information of the molecules involved in the signaling processes (Figure 12). The concentration range used and the time of measurement are central and critical parameters for rational use of salen-manganese complexes in the analysis of hydrogen peroxide-driven processes. In the case of exogenous generation of hydrogen peroxide by GOX and subsequent direct apoptosis induction by hydrogen peroxide, relative high concentrations of EUK-8 (between 2 and 37 μM) were necessary, as well as suitable for inhibition of this rapid process and thus for determining the role of hydrogen peroxide in it. In contrast, analysis of hydrogen peroxide-dependence of autocrine apoptosis induction of transformed cells required much lower concentrations of EUK-8 (below 5 μM) and higher concentrations caused massive apoptosis induction at 27.5 h. Low concentrations of EUK-8 were useful for the demonstration of the dependence of intercellular ROS signaling on hydrogen peroxide, as well as for the demonstration of interference of additional hydrogen peroxide with HOCl signaling (Figure 2B). EUK-8 at the very low concentration of 0.6 μM enabled the inhibitory role of exogenous superoxide anions (due to HOCl/superoxide anion

interaction distant from the cell membrane and thus blunting site-specific HOCl signaling) to be distinguished from the theoretical alternative of HOCl consumption by hydrogen peroxide (Figure 5). In the same experiment, the role of hydrogen peroxide for apoptosis induction was confirmed for high concentrations of XO. These examples show that basic information on the process studied are necessary for the use of the appropriate concentrations of the salen-manganese complex for analysis in order to avoid failure of inhibition due to excess hydrogen peroxide on the one hand and apoptosis induction by the mimetic due to excess of salen manganese complex on the other, thus masking the potential inhibition of the process. Therefore, in the study of most processes, the application of a broad concentration range of the salen-manganese complexes is advised. Induction of apoptosis by higher concentrations of salen-manganese complexes (as seen in Figures 3B and 4) is not due to a nonspecific toxic effects but represents the outcome of complex ROS signaling driven by the salen-manganese complexes. As shown in Figure 4, apoptosis induction by very high concentrations of EUK-8 and EUK-134 precedes and exceeds autocrine apoptotic signaling of transformed cells. Only a well-defined small concentration range of the catalase mimetics allows autocrine apoptosis induction to be inhibited. This example clearly demonstrates that the use of excess EUK-8 or EUK-134 would be misleading in analysis and the use of a broad concentration range of the compounds is necessary in order to obtain clear-cut results. The mechanism underlying apoptosis induction by high concentrations of the salen-manganese compounds seems to involve generation of HOCl by salen-manganese complexes under defined conditions and will be the focus of a separate study. The reverse reaction, *i.e.* decomposition of excess HOCl by salen-manganese complexes is therefore not unexpected (Figure 11) and is in line with published work (27). Our findings allow us to predict that in the presence of hydrogen peroxide, salen-manganese complexes will protect HOCl against reaction with hydrogen peroxide by preferentially decomposing hydrogen peroxide (Figure 2B; (19, 20)), whereas direct reaction with HOCl in the absence of hydrogen peroxide may provoke the decomposition of HOCl. This illustrates again that the interpretation of data obtained by the use of salen-manganese complexes requires the knowledge of the basic partners involved in the signaling reactions in order to obtain the correct conclusions. The powerful catalase mimetic activity of EUK-8 and EUK-134 is not *per se* indicative of the potential involvement of hydrogen peroxide in a specific process studies, as EUK-8 and EUK-134 can also decompose peroxynitrite. It is important to state that this dual activity of the salen-manganese complexes is shared by genuine catalase, which has also been shown to decompose hydrogen peroxide as well as peroxynitrite, with catalase intermediate compound I (CAT $Fe^{IV}=O^{+\bullet}$) formation in both reactions (20, 29, 30). Again, this situation requires the parallel analysis of the source of the substrate in order to obtain an unequivocal result. In the case of intercellular ROS signaling, this can be achieved by testing for the involvement of NO synthase in combination with NADPH oxidase or, alternatively, for the effect of a specific peroxynitrite decomposition catalyst such as FeTPPS. This approach would be indicative of the role of peroxynitrite, whereas a role of NADPH oxidase without a role for NO synthase and without inhibition by FeTPPS would indicate that an inhibitory effect of salen-manganese complexes might be due to an involvement of hydrogen peroxide, the dismutation product of superoxide anions derived from NADPH oxidase. The differentiation between hydrogen peroxide and peroxynitrite-dependent signaling reactions becomes more complex due to the consumption reaction between hydrogen peroxide and NO. This interaction has been repeatedly shown (19, 20, 31). Its detailed mechanism will be presented elsewhere. In this complicated scenario, the site of peroxynitrite generation plays a crucial role. If peroxynitrite is added to the cell system directly, the salen-manganese complex will decompose peroxynitrite as efficiently as hydrogen peroxide. A differentiation between the two substrates therefore seems to be unlikely under these specific experimental conditions. If, however, peroxynitrite is formed exclusively close to the membrane of transformed cells, due to the interaction between NO and superoxide anions, high concentrations of EUK-8 or EUK-134 are required for decomposition of peroxynitrite and protection of the target cells. The requirement for a high concentration of the catalase mimetic under these conditions is due to the specific steric and kinetic situation established by local peroxynitrite generation in the direct vicinity of the membrane. This finding is paralleled by the identical requirement for high catalase requirement for protection against peroxynitrite generated close to the membrane in contrast to peroxynitrite added exogenously to the system (20). The requirement for a high concentration of EUK-8 or EUK-134 to protect against effects of peroxynitrite generated at the membrane allowed us to dissect the complex pattern of hydrogen peroxide and NO interaction. As shown in Figure 9, low concentrations of the salen-manganese complex prevented hydrogen peroxide-dependent consumption of NO and thus enhanced NO/peroxynitrite signaling, whereas high concentrations of the mimetics gradually inhibited NO/peroxynitrite signaling, due to the decomposition of peroxynitrite. Therefore, apoptosis induction mediated by DEA-NONOate in the presence of 1.56 μM EUK-134 (Figure 9B) shows the true dependency of apoptosis on the concentration of DEA-NONOate, whereas apoptosis induction in the control curve also reflects inhibition by cell-derived hydrogen peroxide at low DEA-NONOate concentrations. If, therefore, the curve, measured in the presence of 1.56 μM EUK-134 is taken as a reference curve,

100 μM EUK-134 show inhibition over the whole concentration range of DEA-NONOate. If, however, the control curve is taken as reference, inhibition by EUK-134 in the low concentration range of DEA-NONOate is not overt, as apoptosis induction is blocked by hydrogen peroxide/NO consumption. At low concentrations of EUK-8/EUK-134, the increase of available NO through prevention of its interaction with hydrogen peroxide was dominant over a theoretically possible oxidation of NO by the salen-manganese complex, as recently published (27). Whether oxidation of NO plays an additional and enhancing role for inhibition of NO/peroxynitrite signaling at high concentrations of salen-manganese complexes cannot be deduced from our data, but also cannot be excluded. Intercellular ROS signaling depends on distinct superoxide anion-driven reactions, such as the interaction between superoxide anions with HOCl, in order to generate hydroxyl radicals, or peroxynitrite formation by the interaction of superoxide anions and NO. The published SOD activity of salen-manganese complexes (21, 22) seems not to be sufficiently efficient to interfere with these reactions under the conditions of the signaling system described by us and at the concentrations of the mimetics used. Otherwise, the negative interference of exogenous (not membrane site-specific) superoxide anions on HOCl signaling (Figure 5) should have been inhibited by EUK-8 and the effect of NO/peroxynitrite signaling after addition of an exogenous NO donor to transformed cells (Figure 9) should have been blocked by EUK-8 and EUK-134. Controls performed for this experiment (shown in Figure 8) demonstrate that SOD mimetics such as MnTM-2-PyP are highly efficient SOD mimetics and are superior to the salen-manganese complexes with respect to the analysis of direct superoxide anion involvement in ROS signaling. Taken together, our data demonstrate the great potential of salen-manganese complexes for the analysis of complex intercellular ROS signaling processes, provided they are applied at the correct concentration range for a specific reaction and time window and parallel controls define the major players involved in the signaling process.

Acknowledgements

We thank J. Brandel for valuable help during preparation of the graphs and R. Fröhlich, F. Hettich and M. Lebtig for preparing media, buffer and glassware. This work was supported by a grant from EuroTransBio (ETB1 0315012B)and from EC RiscRad-contract-FI6R-CT-2003-508842. We are grateful for intellectual support by the COST consortium ChemBioRadical (COST Action CM0603).

References

1 Irani K, Xia Y, Zweier JL, Sollott SJ, Der CJ, Fearon ER, Sundaresan M, Finkel T and Goldschmidt-Clermont PJ: Mitogenic signalling by oxidants in *Ras*-transformed fibroblasts. Science *275*: 1649-1652, 1997.

2 Suh Y-A, Arnold RS, Lassegue B, Shi J, Xu X, Sorescu D, Chung AB, Griendling KK and Lambeth JD: Cell transformation by the superoxide-generating oxidase Mox1. Nature *401*: 79-82, 1999.

3 Yang JQ, Li S, Domann FE, Buettner G and Oberley LW : Superoxide generation in v-Ha-*ras*-transduced human keratinocyte HaCaT cells. Mol Carcinogenesis *26*: 180-188, 1999.

4 Heigold S, Sers C, Bechtel W, Ivanovas B, Schäfer R and Bauer G: Nitric oxide mediates apoptosis induction selectively in transformed fibroblasts compared to nontransformed fibroblasts. Carcinogenesis *23*: 929-941, 2002.

5 Mitsushita J, Lambeth JD and Kamata T: The superoxide-generating oxidase Nox1 is functionally required for *Ras* oncogenic transformation. Cancer Res *64*: 3580-3585, 2004.

6 Arnold RS, Shi J, Murad E, Whalen AM, Sun CQ, Palavarapu R, Parthasarathy S, Petros JA and Lambeth JD: Hydrogen peroxide mediates the cell growth and transformation caused by the mitogenic oxidase Nox1. Proc Natl Acad Sci USA *98*: 5550-5555, 2001.

7 Tominaga K, Kawahara T, Sano t, Toida K, Kuwano Y, Sasaki H and Kawai T: Evidence for cancer-associated expression of NADPH oxidase 1 (NOX1)-base oxidase system in the human stomach. Free Radical Biol Med *43*: 1627-1638, 2007.

8 Laurent E, McCoy JW, Maccina RA, Liu W, Cheng GJ, Robine S, Papkoff J and Lambeth JD: NOX1 is overexpressed in human colon cancers and correlates with activating mutations in *K-RAS*. Int J Cancer *123*: 100-107, 2008.

9 Jürgensmeier J, Schmitt CP, Viesel E, Höfler P and Bauer G: TGF-β-treated normal fibroblasts eliminate transformed fibroblasts by induction of apoptosis. Cancer Res *54*: 393-398, 1994.

10 Beck E, Schäfer R and Bauer G: Sensitivity of transformed fibroblasts for intercellular induction of apoptosis is determined by their transformed phenotype. Exp Cell Res *234*: 47-56, 1997.

11 Herdener M, Heigold S, Saran M and Bauer G: Target cell-derived superoxide anions cause efficiency and selectivity of intercellular induction of apoptosis. Free Radical Biol Med *29*: 1260-1271, 2000.

12 Bauer G: Reactive oxygen and nitrogen species: efficient, selective and interactive signals during intercellular induction of apoptosis. Anticancer Res *20*: 4115-4140, 2000.

13 Bauer G: Signaling and proapoptotic functions of transformed cell-derived reactive oxygen species. Prostagl Leukotri Essent Fatty Acid *66*: 41-56, 2002.

14 Bechtel W and Bauer G: Catalase protects tumor cells against apoptosis induction by intercellular ROS signaling. Anticancer Res *29*: 4541-4557, 2009.

15 Bauer G: Low dose radiation and intercellular induction of apoptosis: potential implications for the control of oncogenesis. Int J Radiat Biol *83*: 887-902, 2007.

16 Steinebach C and Bauer G: An alternative signalling pathway based on nitryl chloride during intercellular induction of apoptosis. In Vitro Appl Mol Toxicol *14*: 107-120, 2001.

17 Schimmel M and Bauer G: Proapoptotic and redox state-related signalling of reactive oxygen species generated by transformed fibroblasts. Oncogene *21*: 5886-5896, 2002.

18 Engelmann I, Eichholtz-Wirth H and Bauer G: *Ex vivo* tumor cell lines are resistant to intercellular induction of apoptosis and independent of exogenous survival factors. Anticancer Res *20*: 2361-2370, 2000.

19 Bechtel W and Bauer G: Modulation of intercellular ROS signaling of human tumor cells. Anticancer Res *29*: 4559-4570, 2009.
20 Heinzelmann S and Bauer G: Multiple protective functions of catalase against intercellular apoptosis-inducing ROS signaling of human tumor cells. Biol Chem *391*: 675-693, 2010.
21 Salvemini D, Riley DP and Cuzzocrea S: SOD mimetics are coming of age. Nature Reviews Drug Discovery *1*: 267-374, 2002.
22 Baudry M, Etienne S, Bruce A, Palucki M, Jacobsen E und Malfroy B: Salen-manganese complexes are superoxide dimutase-mimetics. Biochem Biophys Res Commun *192*: 964-968, 1993.
23 Gonzalez PK, Zhuang J, Doctrow SR, Malfroy B, Benson PF, Menconi MJ und Fink MP: EUK-8, a synthetic superoxide dismutase and catalase mimetic, ameliorates acute lung injury in endotoxemic swine. J Pharmacol Exp Ther *275*: 798-806, 1995.
24 Doctrow SR, Huffman K, Bucay Marcus C, Tocco G, Malfroy E, Adinolfi C, Kruk H, Baker K, Lazarowych N, Mascarenhas J and Malfroy B: Salen-manganese complexes as catalytic scavengers of hydrogen peroxide and cytoprotective agents: structure-activity relationship studies. J Med Chem *45*: 4549-4558, 2002.
25 Abashkin YG and Burt SK: (Salen)MnIII compounds as nonpeptidyl mimics of catalase. Mechanism-based tuning if catalase activity: a theoretical study. Inorg Chem *44*: 1425-1432, 2005.
26 Watanabe T, Owada S, Koboyashi HP, Kawakami H, Nagaoka S, Murakimi E, Ishiuchi A, Enomoto T, Jinnouchi Y, Sakurai J, Tobe N, Kozumi S, Shimamura T, Asakura T, Nakano H and Otsubo T: Protective effects of MnM2Py4P and Mn-salen against small bowel ischemia/reperfusion injury in rats using an *in vivo* and an *ex vivo* electron paramagnetic resonance technique with a spin probe. Transplant Proc *39*: 3002-3006, 2007.
27 Sharpe MA, Ollosson R, Stewart VC and Clark JB: Oxidation of nitric oxide by oxomanganese-salen complexes: a new mechanism for cellular protection by superoxide dismutase/catalase mimetics. Biochem J *366*: 97-107, 2002.
28 Bauer G, Höfler P and Simon M: Epstein-Barr virus induction by a serum factor II. Purification of a high molecular weight protein that is responsible for induction. J Biol Chem *257*: 11405-11410, 1982.
29 Gebicka L and Didik J: Catalytic scavenging of peroxynitrite by catalase. J Inorg Biochem *103*: 1375-1379, 2009.
30 Kono Y, Yamasaki T, Ueda A and Shibata H: Catalase catalyzes peroxynitrite-mediated phenolic nitration. Biosci Biotechnol Biochem *62*: 448-452, 1998.
31 Haberstroh K, Heigold S and Bauer G: Transformed cell-derived reactive oxygen species support and inhibit nitric oxide-mediated apoptosis induction. Int J Oncol *21*: 145-151, 2002.

Received July 14, 2010
Revised September 7, 2010
Accepted September 14, 2010